TOXICOLOGICAL SCIENCES **128(2)**, 326–333 (2012)
doi:10.1093/toxsci/kfs151
Advance Access publication April 26, 2012

A Single Neonatal Exposure to Aflatoxin B_1 Induces Prolonged Genetic Damage in Two Loci of Mouse Liver

Roongtiwa Wattanawaraporn,*,† Leslie L. Woo,* Crystal Belanger,* Shiou-chi Chang,* Jillian E. Adams,* Laura J. Trudel,* Jason T. Bouhenguel,* Patricia A. Egner,‡ John D. Groopman,‡ Robert G. Croy,* John M. Essigmann,* and Gerald N. Wogan*,[1]

*Department of Biological Engineering and Department of Chemistry, Massachusetts Institute of Technology, Cambridge, Massachusetts 02139; †Graduate Program in Applied Biological Sciences, Chulabhorn Graduate Institute, Bangkok 10210, Thailand; and ‡Department of Environmental Health Sciences, Johns Hopkins Bloomberg School of Public Health, Baltimore, Maryland 21205

[1]To whom correspondence should be addressed. Fax: (617) 253-5445. E-mail: wogan@mit.edu.

Received October 24, 2011; accepted April 14, 2012

Aflatoxin B_1 (AFB_1) is a risk factor for hepatocellular carcinoma in humans. Infant, but not adult, mice are sensitive to AFB_1-induced liver carcinogenesis; a single dose during the neonatal period leads to hepatocellular carcinoma in adulthood. Earlier work defined the mutational spectrum in the *gpt* gene of *gpt* delta B6C3F1 mice 3 weeks after exposure to aflatoxin. In the present study, we examined the *gpt* spectrum 10 weeks postdosing and expanded the study to examine, at 3 and 10 weeks, the spectrum at a second locus, the *red/gam* genes of the mouse λEG10 transgene. Whereas the *gpt* locus is typically used to define local base changes, the *red/gam* genes, via the Spi^- assay, often are used to detect more global mutations such as large deletions and rearrangements. Three weeks after dosing with AFB_1, there was a 10-fold increase over the control in the Spi^- mutant fraction (MF) in liver DNA; after 10 weeks, a further increase was observed. The MF in the *gpt* gene was also increased at 10 weeks compared with the MF at 3 weeks. No gender-specific differences were found in the Spi^- or *gpt* MFs. Whereas Spi^- mutations often signal large genetic changes, they did not in this specific case. The Spi^- spectrum was dominated by GC to TA transversions, with one exceptionally strong hotspot at position 314. Using two genetic loci, the data show a strong preference for the induction of GC to TA mutations in mice, which is the dominant mutation seen in people exposed to aflatoxin.

Key Words: **aflatoxin B_1; hepatocellular carcinoma; mutation; infant mouse.**

In mice, the ability of aflatoxin B_1 (AFB_1) to produce covalent adducts in liver DNA of infant and adult animals differs, respectively, by 20-fold (Shupe and Sell, 2004) with correspondingly different incidences of hepatocellular carcinoma (HCC) (Busby and Wogan, 1984). AFB_1 is a potent hepatocarcinogen in infant mice, but older mice are refractory to its carcinogenic effects because of changes in AFB_1 metabolism that reduce its ability to cause genotoxic damage (Dycaico *et al.*, 1996; Hayes *et al.*, 1991). In infant B6C3F1 mice, a single dose of AFB_1 produces a high incidence of HCC in adult male mice but not in female mice (Vesselinovitch *et al.*, 1972). This gender disparity in HCC is seen in other rodent models and also parallels human epidemiological data. In humans, there is an established relationship between exposure to AFB_1, levels of AFB_1-DNA adducts in urine, and the incidence of HCC (Groopman *et al.*, 2008). Furthermore, the incidence of HCC in men is about two to four times higher than in women (El-Serag and Rudolph, 2007). Elucidating the molecular details underlying age, species, and gender differences in carcinogenesis is central to the development of effective preventive strategies.

Carcinogenesis is characterized by sequential alterations in gene expression involving genetic and epigenetic mechanisms that can be induced by endogenous and/or environmental factors. Mutations produced by genotoxicants are essential for initiation of the carcinogenic process by most chemical carcinogens. Several studies have characterized the number and types of mutations produced in animal models shortly after treatment with AFB_1 and other genotoxic carcinogens (Chen *et al.*, 2010; Woo *et al.*, 2011). However, little is known about the numbers and types of mutations that are present in the liver over the extended period required for the development of HCC.

Integrated bacterial reporter genes in transgenic mice have enabled characterization of somatic mutations that occur spontaneously or are produced by genotoxins that can cause cancer. Using transgenic *gpt* delta B6C3F1 mice, we recently examined the number and types of mutations produced in the liver after treatment of newborn animals with AFB_1 (Woo *et al.*, 2011). The *gpt* assay detected base pair substitutions, single base insertions, and small deletions, all of which have been associated with tumor development. Three weeks after AFB_1 administration, the *gpt* mutant fraction (MF) in the liver was increased approximately 20-fold in both males and females, indicating that shortly after exposure both sexes were at comparable risk of tumor-initiating mutations from AFB_1-induced DNA damage.

The purpose of the present study was to assess the capability of AFB_1 to generate other types of DNA sequence changes including those driven by nonhomologous recombination

in vivo by analyzing the Spi$^-$ (*S*ensitive to *P*2 *I*nhibition) phenotype resulting from the disruption of *red* and *gam* genes in the λEG10 transgene of *gpt* delta B6C3F1 mice. We also extended our previous studies to demonstrate the persistence of base substitutions, insertions, and deletions in liver of both sexes following puberty. Point mutations were found to occur most frequently; however, AFB$_1$ was also a potent inducer of Spi$^-$ mutants, which were molecularly characterized in this work.

MATERIALS AND METHODS

Chemicals. AFB$_1$, DMSO and 6-thioguanine (6-TG) were obtained from Sigma Chemical Co. (St Louis, MO). All other chemicals and media were obtained from commercial suppliers and used as provided.

Animals and treatments. Female *gpt* delta C57BL/6J mice (Nohmi *et al.*, 1996) were crossed with male C3H/HeJ mice to obtain an F1 that was hemizygous for the *gpt* transgene on chromosome 17. Four-day-old B6C3F1 animals were treated with AFB$_1$ dissolved in DMSO administered via ip injection. Infant mice were weaned at 21 days. Animals were fed AIN93G diet *ad libitum*. All procedures involving animals were approved by the MIT Committee on Animal Care.

Analysis of covalent AFB$_1$ adducts in liver DNA. Liver DNA was isolated from AFB$_1$-treated mice and AFB$_1$-DNA adducts hydrolyzed using previously described procedures (Woo *et al.*, 2011). Internal $^{15}N_5$-guanine-derived standards for both AFB$_1$-N^7-guanine and AFB$_1$-FAPY were added after hydrolysis of AFB$_1$-DNA adducts to permit quantitative analysis by isotope dilution mass spectrometry. DNA adducts were separated by ultra-high performance liquid chromatography and injected for MS/MS analysis. The protonated parent ion of the AFB$_1$-N^7-guanine adduct (*m/z* 480.1) was selected and subjected to collision-induced fragmentation producing a *m/z* 152 product ion that was monitored to quantify adduct levels. The AFB$_1$-FAPY adduct was quantified by selection of the *m/z* 498 parent ion and monitoring the collision-induced product ion *m/z* 452 (Egner *et al.*, 2006).

Mutation assays. The *gpt* and Spi$^-$ assays were performed using genomic DNA isolated from mice injected with AFB$_1$ or vehicle (DMSO). Genomic DNA was extracted from 25 mg liver tissue using a RecoverEase DNA Isolation Kit (Agilent Technologies, Santa Clara, CA); subsequently, λEG10 phages were packaged *in vitro* from the genomic DNA using Transpack Packaging Extract (Agilent Technologies) following the manufacturer's instructions. The selection of 6-TG-resistant mutants and sequencing of the *gpt* gene were performed as described previously (Woo *et al.*, 2011).

The Spi$^-$ assay was performed by infecting XL1 Blue MRA *Escherichia coli* with rescued phage to estimate the total number of phage and XL1 Blue MRA (P2) *E. coli* to enumerate phage with the Spi$^-$ phenotype. Mutants were confirmed by growth on WL95 (P2) and XL1 Blue MRA *E. coli* strains. The Spi$^-$ mutant fraction was calculated as the number of confirmed mutants divided by the total number of packaged phage (Nohmi *et al.*, 1996).

Analysis of Spi$^-$ mutants. Spi$^-$ phage were used to infect *E. coli* LE392 and incubated until lysis. Phage DNA was isolated from the Spi$^-$ lysate and a 5 kb segment containing the *red* and *gam* genes was amplified by PCR using primers: (5′-CTCTCCTTTGATGCGAATGCCAGA-3′) and (5′-GGAGTAATTATGCGGAACAGAATCATGC-3′). The PCR products were analyzed by agarose gel electrophoresis and purified for sequencing (QIAquick PCR Purification Kit, Qiagen). Sequencing of the *gam* gene was performed at the Biopolymers Facility at Harvard Medical School (Boston, MA) using the primer (5′-CCACTTTTATTGGCGATGAAAAGATGTTC-3′). Sequences were aligned with the λ *gam* gene (NC_001416) using NCBI Nucleotide Blast.

Statistical analyses. Mutational spectra were compared using the Adams-Skopek test (Adams and Skopek, 1987; Cariello *et al.*, 1994). The Mann-Whitney nonparametric test was used to determine statistical significance of differences in MF.

RESULTS

AFB$_1$ adducts in liver DNA 3 weeks after treatment. The experimental protocol used in this investigation is shown in Figure 1. Mice were injected ip with a single dose of 6 mg/kg AFB$_1$ on day 4 after birth. AFB$_1$-DNA adduct levels in liver were analyzed 3 weeks later as described earlier. Our previous investigation quantified adduct levels up to 48 h after AFB$_1$ was administered (Woo *et al.*, 2011). Here we extended the period of observation to determine whether the persistent and more mutagenic AFB$_1$-FAPY adduct had the potential to increase the mutation frequency in liver cells over an extended period. The previous analyses showed that both the AFB$_1$-N^7-guanine adduct and the imidazole ring-opened form (AFB$_1$-FAPY) were present 48 h after dosing (Woo *et al.*, 2011). Three weeks after dosing, the AFB$_1$-N^7-guanine adduct was undetectable, whereas amounts of the highly mutagenic AFB$_1$-FAPY persisted in liver DNA at a level of 1 adduct/10^7 nucleotides. This result suggested that additional mutations could be induced over the subsequent period of liver cell proliferation and prompted us to extend our original analyses of mutations in the *gpt* transgene.

The time point of 3 weeks in our previous study was chosen because by that age the liver had completed its initial phase of rapid growth during which mutations could be created through errors in repair or replication of DNA containing AFB$_1$ adducts. In the present study, the "fixation/expression" period was extended to determine how the mutant fraction in liver changed between 3 and 10 weeks after dosing. We recorded liver weight as a measure of age-related changes in cell proliferation and growth. At the time of AFB$_1$ administration on day 4 after birth, the liver in males and females weighed 54 ± 11 mg and 48 ± 13 mg, respectively; two days later (day 6), liver weights had increased significantly in both males (80 ± 23 mg) and females (74 ± 17 mg). At 25 days of age, which was 21 days after treatment, liver weights had increased by about 10-fold in both sexes (male 815 ± 73 mg; female 720 ± 50 mg). Thereafter, the rate of increase in liver weight slowed, nearly doubling during

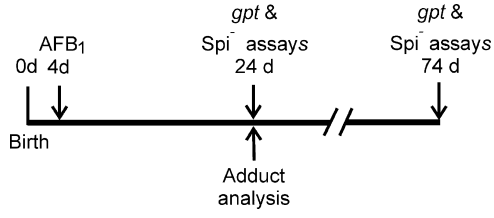

FIG. 1. Experimental scheme for treatment of 4-day old *gpt* delta B6C3F1 mice with 6 mg/kg AFB$_1$, analysis of DNA adducts and *gpt* and Spi$^-$ mutation assays.

the subsequent 7 weeks and attaining an average weight of 1400 ± 374 mg in males and 970 ± 340 mg in females.

Mutation fraction in the gpt *gene of AFB_1-treated infant mice.* Three and 10 weeks after treatment with a single dose of 6 mg/kg AFB_1, λ transgenes were recovered from liver DNA by *in vitro* packaging. Growth of the λ phage on *E. coli* YG6020 expressing Cre recombinase produced chloramphenicol (CM)-resistant plasmids. Mutations in the *gpt* gene resulted in additional resistance to 6-TG. Tables 1 and 2 show the numbers of colonies resistant to CM and CM + 6-TG for each animal and the calculated *gpt* mutant fractions.

Tables 1 and 2 (also Fig. 2) depict that the average *gpt* MFs in the liver in AFB_1-treated mice was greater at 10 weeks than at 3 weeks, with the increase in males ($p = 0.02$) during this 7-week period being greater than that found in females ($p = 0.07$). In DMSO-treated controls, the *gpt* MFs also increased, but the differences did not reach statistical significance (males $p = 0.06$; females $p = 0.4$); at 10 weeks, the *gpt* MF in the livers of males and females was the same ($p = 0.55$).

TABLE 1
***gpt* Mutant Fractions in Liver of *gpt* Delta B6C3F1 Mice 3 Weeks After Treatment With DMSO or AFB_1**

Treatment	Animal no.	Sex	CM^R colonies ($\times 10^6$)	6-TGR colonies	Mutant fraction ($\times 10^{-5}$)	Mean ± SD ($\times 10^{-6}$)
DMSO	6	M	1.01	3	0.30	4.0 ± 2.3
	9	M	1.41	9	0.66	
	12	M	1.97	10	0.51	
	15	M	1.47	2	0.14	
	7	F	1.94	10	0.52	7.7 ± 4.3
	8	F	0.31	3	1.10	
	10	F	1.50	17	1.17	
	20	F	1.15	3	0.29	
AFB_1	26	M	1.27	177	13.4	136 ± 2
	30	M	1.44	171	13.4	
	23	M	1.80	207	11.5	
	24	M	1.63	262	16.2	
	22	F	1.34	217	16.2	153 ± 3
	25	F	1.39	173	12.8	
	32	F	1.29	233	18.5	
	35	F	1.23	163	13.6	

Note. CM^R = chloramphenicol resistant; 6-TGR = 6-thioguanine resistant.

TABLE 2
***gpt* Mutant Fractions in Liver of *gpt* Delta B6C3F1 Mice 10 Weeks After Treatment With DMSO or AFB_1**

Treatment	Animal no.	Sex	CM^R colonies ($\times 10^6$)	6-TGR colonies	Mutant fraction ($\times 10^{-5}$)	Mean ± SD ($\times 10^{-6}$)
DMSO	110	M	1.90	21	1.11	12.5 ± 2.3
	111	M	1.07	12	1.12	
	112	M	1.32	20	1.51	
	113	F	1.18	17	1.44	10.0 ± 4.7
	114	F	3.18	16	0.50	
	115	F	1.40	17	1.22	
AFB_1	103	M	0.71	121	17.0	183 ± 19
	105	M	1.51	286	19.0	
	131	M	1.53	315	20.5	
	132	M	0.49	78	15.8	
	133	M	1.07	206	19.3	
	101	F	0.87	109	12.5	191 ± 40
	102	F	1.97	433	22.0	
	120	F	2.39	443	18.5	
	122	F	1.26	260	20.6	
	130	F	1.03	227	22.1	

Note. CM^R = chloramphenicol resistant; 6-TGR = 6-thioguanine resistant.

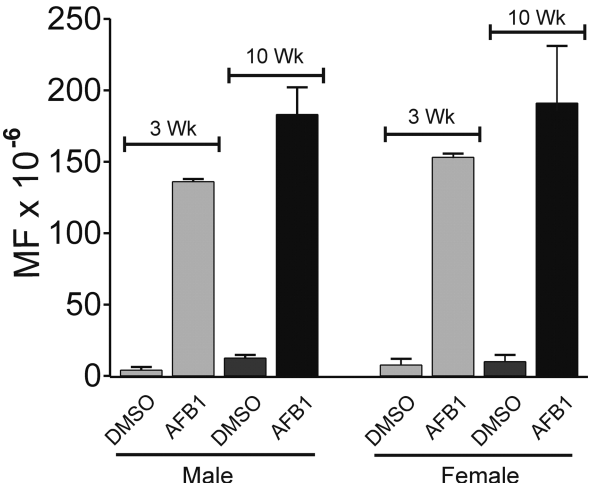

FIG. 2. *gpt* MF in *gpt* delta B6C3F1 mouse liver 3 weeks or 10 weeks after treatment with 6 mg/kg AFB_1 or vehicle (DMSO) at day 4 after birth.

Sequencing of the 456 bp *gpt* gene in 157 6-TG-resistant colonies revealed similar types and positions of mutations at 3 weeks and 10 weeks. Table 3 summarizes the types of mutations found in the *gpt* gene in livers of 17 AFB_1-treated mice (males and females) 10 weeks after treatment. As we previously observed, 3 weeks after AFB_1 treatment, the G:C to T:A transversion was the most frequent type of mutation present (55%) (Woo *et al.*, 2011). Figure 3 shows the distribution of base pair changes, insertions, and small deletions in the *gpt*

TABLE 3
Summary of Mutation Types in the *gpt* Gene of Male and Female *gpt* Delta B6C3F1 Mice 10 Weeks After Treatment With a Single 6 mg/kg Dose of AFB_1

	AFB_1	
Mutation types	Male	Female
Transition:		
G:C to A:T	11 (13)	9 (12)
A:T to G:C	0	0
Transversion:		
G:C to T:A	58 (71)	50 (67)
G:C to C:G	6 (7)	4 (5)
A:T to T:A	3 (4)	5 (7)
A:T to C:G	0	0
Deletion:		
1 bp	2 (2)	4 (5)
> 1 bp	0	0
Insertion	2 (2)	3 (4)
Total number of mutants	55 (100)	75 (100)

Note. The percentage of each type of mutation is shown in parentheses.

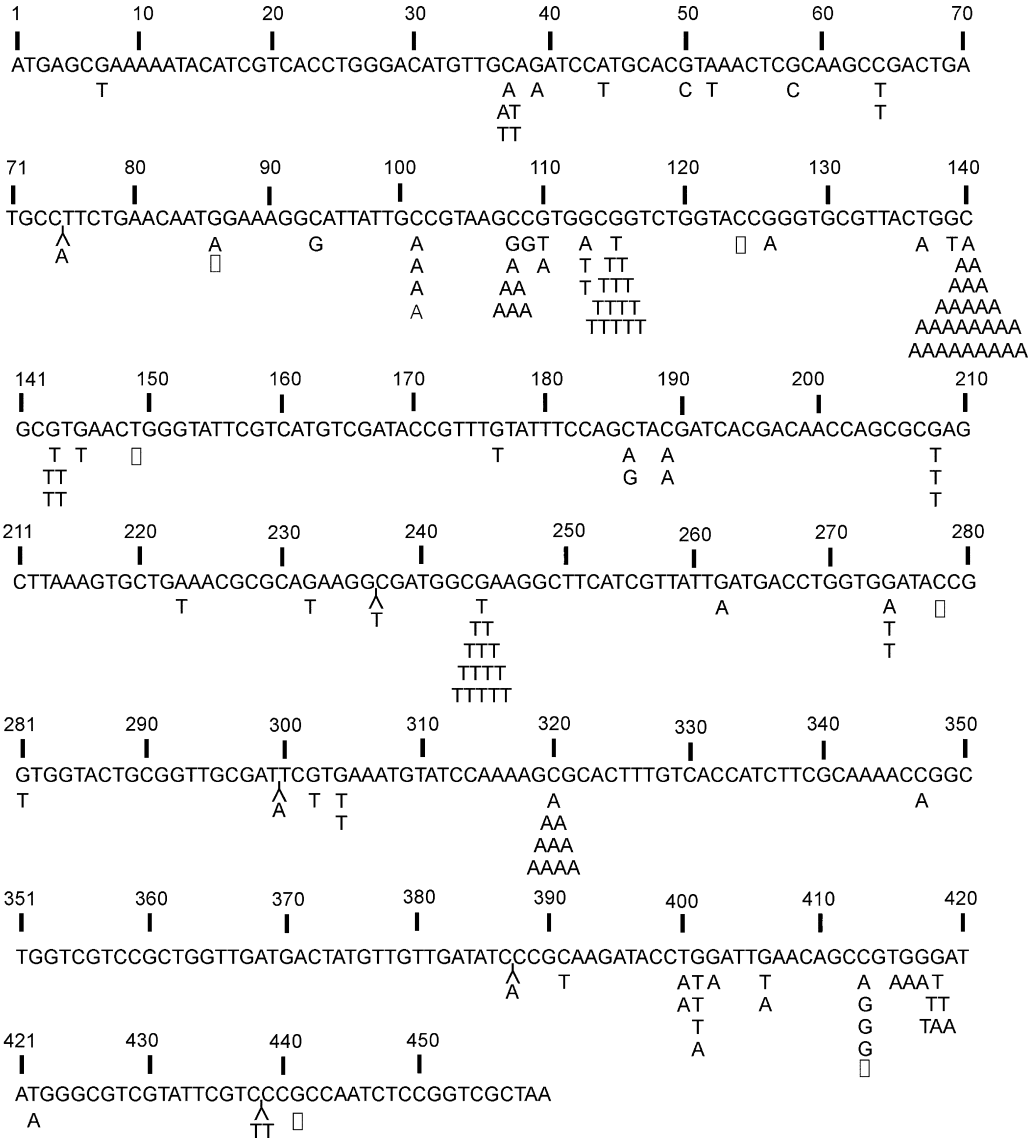

FIG. 3. Distribution of mutations in the *gpt* gene in liver of *gpt* delta B6C3F1 mice 10 weeks after treatment with 6 mg/kg AFB$_1$. Base substitutions are indicated by symbols Y = insertion; □ = deletion.

gene at 10 weeks. Monte Carlo-based analysis revealed no differences between the *gpt* mutational spectra at 3 or 10 weeks after treatment ($p > 0.05$) (Adams and Skopek, 1987).

AFB$_1$-Induced Spi$^-$ Mutations in Liver. The Spi$^-$ assay is sensitive to mutations in the *red* and *gam* genes of the λEG10 transgene (Masumura *et al.*, 2000). Figure 4, along with the data in Tables 4 and 5, illustrates that at 3 and 10 weeks after AFB$_1$ treatment there was a 10- to 20-fold increase in the Spi$^-$ MF in liver DNA compared with vehicle-treated control mice. Equal fractions of Spi$^-$ mutations were found in male and female mice at 3 weeks. At 10 weeks, the Spi$^-$ MF in AFB$_1$-treated mice was increased significantly in both males ($p = 0.004$) and females ($p = 0.02$) compared with the 3-week MF.

Spi$^-$ mutants from 10-week mice were first characterized by PCR amplification of a 5 kb segment of the λEG10 transgene containing both the *gam* and *red* genes. All of the mutants produced a full-length 5 kb PCR product indicating that there were no large deletions or other types of rearrangements in the *gam* and *red* gene coding sequences. Mutations in the *gam* gene alone can show the Spi$^-$ phenotype (Singer, 1971). Therefore, we decided to perform sequence analysis of *gam* to identify any base substitutions or small insertions/deletions characteristic of those produced by AFB$_1$. Figure 5 shows the sequence changes that were identified in the *gam* gene of Spi$^-$ phage isolated from AFB$_1$-treated mice and DMSO-treated controls. Ninety-six Spi$^-$ λEG10 phage were sequenced from 10 AFB$_1$-treated mice. Only 14 mutants were available for sequence analysis from the 6 control mice treated with DMSO. Base pair substitutions

TABLE 4
Spi Mutant Fractions in Liver of *gpt* Delta B6C3F$_1$ Mice 3 Weeks After Treatment With DMSO or AFB$_1$

Treatment	Animal no.	Sex	Plaques ($\times 10^6$)	Plaques (P2) (Spi$^-$)	Mutant fraction ($\times 10^{-5}$)	Mean ± SD ($\times 10^{-6}$)
DMSO	6	M	0.78	1	0.13	1.8 ± 0.9
	9	M	0.75	2	0.28	
	12	M	0.88	2	0.24	
	15	M	1.09	1	0.09	
	7	F	1.03	2	0.19	3.4 ± 1.5
	8	F	1.15	4	0.35	
	10	F	1.10	6	0.55	
	20	F	1.12	3	0.27	
AFB$_1$	23	M	1.03	30	2.96	33.8 ± 14
	34	M	0.32	12	3.77	
	26	M	0.61	31	5.04	
	30	M	0.46	8	1.75	
	22	F	1.57	52	3.38	34.3 ± 9.7
	25	F	1.34	54	4.00	
	32	F	1.01	16	2.09	
	35	F	1.54	65	4.25	

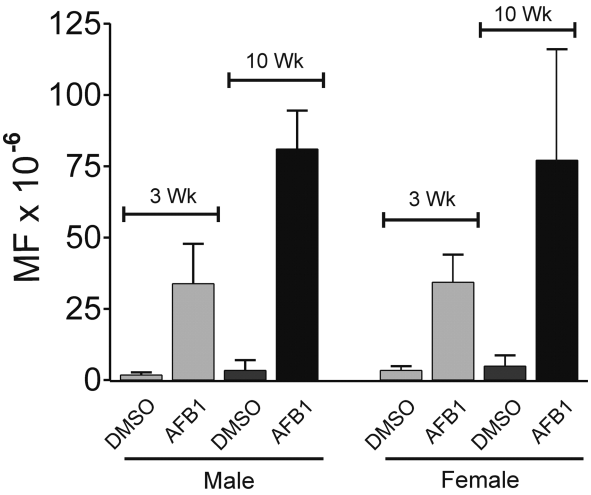

FIG. 4. Spi$^-$ MF in *gpt* delta B6C3F1 mouse liver 3 weeks or 10 weeks after treatment with 6 mg/kg AFB$_1$ or vehicle (DMSO) at day 4 after birth.

were once again the predominant type of mutation, representing 88% of total mutations in AFB$_1$-treated mice. There were no significant gender differences either in the type of mutation in the *gam* gene (Table 6). The C:G to A:T transversion mutation at nucleotide 314 is a hot spot that was found in all 10 AFB$_1$-treated mice analyzed at 10 weeks, representing approximately 50% of the sequenced mutants. The most plausible explanation for this mutation is the formation of an AFB$_1$-Gua adduct on the G-containing strand. Frameshifts resulting from single base pair deletions or insertions represented the next most abundant class of mutations (22% of total). Single base pair deletions predominated in limited number of mutants available for analysis in the 10-week control group.

TABLE 5
Spi Mutant Fractions in Liver of *gpt* Delta B6C3F1 Mice 10 Weeks After Treatment With DMSO or AFB$_1$

Treatment	Animal no.	Sex	Plaques ($\times 10^6$)	Plaques (P2) (Spi$^-$)	Mutant fraction ($\times 10^{-5}$)	Mean ± SD ($\times 10^{-6}$)
DMSO	110	M	2.26	2	0.09	3.4 ± 3.6
	111	M	2.14	4	0.19	
	112	M	0.53	4	0.75	
	113	F	2.11	12	0.57	4.9 ± 3.8
	114	F	2.40	2	0.08	
	115	F	1.91	16	0.84	
AFB$_1$	103	M	0.69	58	8.37	81.0 ± 13.5
	105	M	0.57	59	10.30	
	131	M	1.45	112	7.71	
	132	M	1.02	71	6.94	
	133	M	0.82	59	7.18	
	101	F	0.97	42	4.35	77.1 ± 38.9
	102	F	0.62	22	3.58	
	120	F	3.14	160	5.09	
	122	F	0.98	72	7.32	
	130	F	0.72	95	13.2	

DISCUSSION

Cancer development involves the acquisition of proliferative and invasive phenotypes through the accumulation of genetic variation spontaneously or through exposures to environmental carcinogens. The multiple genetic changes associated with carcinogenesis include point mutations, chromosomal rearrangements, and changes in gene copy number (Futreal *et al.*, 2004). AFB$_1$, one of the most potent known liver carcinogens in humans and animal models, has been shown to be a potent mutagen in bacterial and mammalian cells. Previous work using

TABLE 6
Summary of Mutation Types in the *gam* Gene of Male and Female *gpt* Delta B6C3F1 Mice 10 Weeks After Treatment With a Single 6 mg/kg Dose of AFB$_1$

Mutation types	AFB$_1$ Male	AFB$_1$ Female	DMSO[a]
Transition:			
G:C to A:T	1 (3)	1 (2)	3
A:T to G:C	0 (0)	0 (0)	0
Transversion:			
G:C to T:A	27 (67)	40 (71)	1
G:C to C:G	0 (0)	2 (5)	0
A:T to T:A	0 (0)	1 (2)	1
A:T to C:G	0 (0)	0 (0)	0
Deletion			
1 bp	11 (27)	10 (18)	8
> 1 bp	0 (0)	0 (0)	0
Insertion	1 (3)	1 (2)	1
Total number of mutants	40 (100)	56 (100)	14

Note. The percentage of each type of mutation is shown in parentheses.
[a]Because few mutants were available for analysis, data from male and female mice were combined.

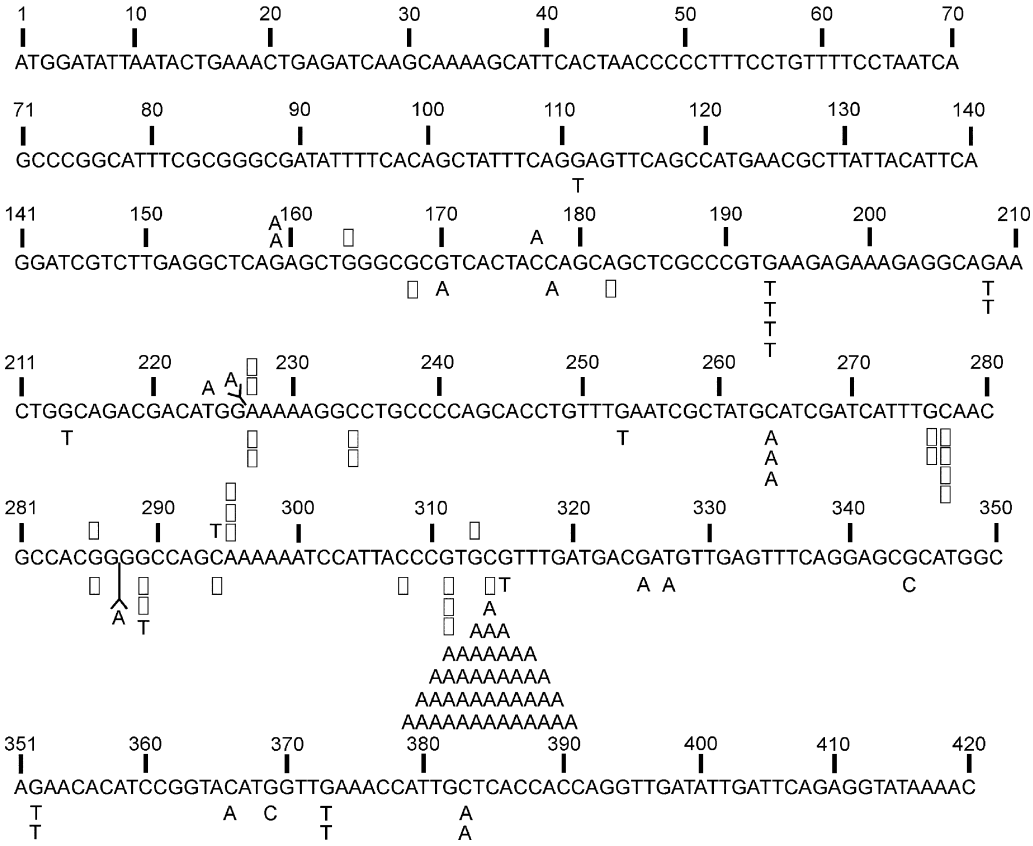

FIG. 5. Distribution of mutations in the *gam* gene in liver of *gpt* delta B6C3F1 mice 10 weeks after treatment with 6 mg/kg AFB$_1$. Base substitutions are indicated by symbols Y = insertion; □ = deletion. Mutations in DMSO-treated mice are shown above the sequence; AFB$_1$-induced mutations are shown below.

bacterial reporter genes in transgenic mice established that neonatal exposure to AFB$_1$ leads to a 20-fold increase in the frequency of point mutations in the *gpt* gene in the liver (Chen *et al.*, 2010; Woo *et al.*, 2011). In the present investigation, we studied the ability of AFB$_1$ to induce mutations in the *gam* and *red* genes of a λEG10 reporter in mouse liver. Mutations in these genes produce the Spi$^-$ phenotype that can be identified by the ability to grow on P2 lysogenic *E. coli* strains. This assay is sensitive to large deletions and rearrangements in the *gam* and *red* genes as well as small deletions, insertions, and base pair substitutions that disrupt transcription and translation of these genes.

In conjunction with the results of our previous study, the findings in the present study establish the ability of AFB$_1$ to induce a broad range of mutation types in the liver DNA, including base pair substitutions and frameshifts resulting from small deletions and insertions. Earlier analyses showed a 13- to 15-fold increase in the MF of the *gpt* transgene at 3 weeks after treatment of 4-day-old mice (Woo *et al.*, 2011); our present findings show that the MF continued to increase up to 20-fold over DMSO-treated controls at 10 weeks thereafter. These results are in agreement with another study that found a 22-fold increase in base substitution and frameshift mutations in the *cII* transgene of neonatal Big Blue B6C3F1 mice 6 weeks after treatment with AFB$_1$ (Chen *et al.*, 2010). The slower increase in MF in the liver from 3 to 10 weeks was very likely due to the decrease in growth rate of the liver after 3 weeks. Liver weight increased approximately 10-fold during the initial 3-week period, and subsequently doubled in size over the next 7 weeks. Cell proliferation provides opportunities for fixation of mutations at damaged sites in DNA through replication errors. Reynolds *et al.* (2004) reported a 27-fold difference in the proliferation index between 4-week and 12-week-old B6C3F1 mice. Thus, during the initial 3-week period, a greater number of AFB$_1$-DNA adducts are present along with greater opportunity for them to cause mutations when cells are in S-phase during this period of rapid liver growth.

The strong mutagenic signal in the Spi$^-$ assay from the liver of AFB$_1$-treated animals is particularly noteworthy. The sequence characteristics of deletions found in *gpt* delta mice after treatment with various agents include –1 bp frameshifts and larger deletions (> 10 kb) containing junction sequences of limited homology that could result from end joining of double strand breaks (Horiguchi *et al.*, 2001; Masumura *et al.*, 2000; Nohmi *et al.*, 1999). The molecular characteristics of the Spi$^-$ mutants from the liver of AFB$_1$-treated mice differ from those found in the aforementioned studies. In the present work on aflatoxin, there were some small deletions and frameshifts observed, but point mutations were more common.

A significant number of base substitutions resulted in the appearance of a stop codon in the *gam* gene, which presumably resulted in a halt in translation in both the *gam* and the contiguous *redAB* genes. Approximately 50% of all base substitution mutations (44 out of 98 sequenced mutations) were found at a single site: the C:G to A:T transversion that occurred at base pair 314. This mutation was not seen among the 15 Spi$^-$ mutants analyzed from DMSO-treated animals, which would indicate that it is a hot spot for AFB_1-induced mutations. This transversion mutation in the *gam* gene results in the substitution of glutamate for an alanine residue that is located in one of the two small helices of the gam protein that functions to anchor larger helical regions for proper binding to the RecBCD complex (Court *et al.*, 2007). The charged glutamate residue may prevent this interaction. Inhibition of the RecBC complex by gam is required for initiation of the rolling circle mode of lambda replication that generates linear concatemers of DNA that can be packaged into infectious phage (Furth and Wickner, 1983). Gam$^-$ phage are confined to the closed-circular form of replication, producing single circular genomes that are not substrates for packaging and consequently are unable to produce plaques. Recombination between circles, however, produces dimers that can be packaged to form infectious progeny. The λEG10 genome contains several Chi sequences that promote recombination by RecBC, facilitating the concatenation of circular genomes and formation of infections particles by gam$^-$ phage (Smith, 1983). This could partly explain our observation of the Spi$^-$ phenotype resulting from the transversion at base pair 314. However, a full explanation will require a better understanding of the basis for Spi$^-$ selection on P2 lysogenic strains. The strong mutagenicity of AFB_1 at base pair 314 may result from its preferential reaction with AFB_1-8,9-oxide, lack of repair, or susceptibility to replication errors. It is also possible, however, that unexpected variables in the conditions used for selection of the Spi$^-$ phenotype are responsible for the apparent prevalence of this mutant in AFB_1-treated animals.

Aflatoxin DNA adducts that could be responsible for these mutations include AFB_1-N^7-Gua and the multiple AFB_1-FAPY adducts. These adducts block replication in *in vitro* assays (Johnston and Stone, 2000; Levy *et al.*, 1992; Refolo *et al.*, 1985). AFB_1-FAPY exists in two rotameric forms (major and minor), which differ substantially with respect to lethal and mutagenic potencies in a bacterial reporter system. The major adduct is a particularly strong block for replication by both normal and bypass DNA polymerases, whereas the minor adduct is most potent at causing base substitutions (Smela *et al.*, 2002), specifically G to T transversions. The presence of AFB_1-FAPY in liver DNA 3 weeks after dosing indicates that this highly persistent adduct has multiple opportunities to cause genetic alterations over an extended period of time during hepatocarcinogenesis.

The increase in the Spi$^-$ MF (10-fold) was a little less than half that of the *gpt* MF (20-fold) measured at 10 weeks of age (see Figs. 2 and 4). It is difficult to compare mutational potencies in different loci, especially in loci that encode such disparate functions as those of the *gpt* and *gam* genes. Nevertheless, the data from these two loci support the view that aflatoxin is a good point mutagen. If it induced frequent more global genetic changes, we would have expected to have seen such mutagenic events among the sequenced Spi$^-$ mutants. In this respect, the types of Spi$^-$ mutants induced by AFB_1 were similar to those reported for 2-amino-1-methyl-6-phenylimidazo[4,5-*b*]pyridine (PhIP) and aminophenylnorharman, which were dominated by small deletions and single base substitutions (Masumura *et al.* 1999, 2003). The absence of large deletions and rearrangements in the *gam* and *red* genes of Spi$^-$ phage in our experiments is in contrast to the reported ability of AFB_1 to cause these types of recombinant-driven changes in yeast (Sengstag *et al.*, 1996) and lymphoid cells in culture (Preisler *et al.*, 2000; Stettler and Sengstag, 2001) as well as reports of its ability to cause micronuclei and sister chromatid exchanges (Busby and Wogan, 1984). Further studies will be required to clarify these apparent discrepancies to understand the role of clastogenic activities of AFB_1 in HCC.

The infant mouse model provides a unique environment in which to investigate the extended process of carcinogenesis following a single exposure to a carcinogen such as AFB_1. A significant finding in this study is the absence of gender differences in *gpt* or Spi$^-$ MFs in liver DNA up to 10 weeks after treatment. On this basis, it would appear that the potential for initiation of HCC development exists in animals of both sexes; eventually, however, female mice develop a much lower incidence of HCC than do males (Vesselinovitch *et al.*, 1972). If formation of mutations and adducts are central to carcinogenesis, this study helps to identify periods later than 10 weeks as the critical periods in defining the sex differences in carcinogenic outcome. In rodent models of HCC, development of premalignant lesions and their rate of progression to malignancy can be modulated by sex hormones and tumor-promoting cytokines (Maeda *et al.*, 2005). Cytokine expression by injured hepatocytes results in the recruitment of inflammatory cells that aid in the process of tumor development (He *et al.*, 2010). The discovery that cytokine expression can be suppressed by estrogenic hormones provides one possible mechanism responsible for the gender difference in incidence of chemically induced HCC in rodents (Naugler *et al.*, 2007). Despite a wealth of information, it is still unclear how the inflammatory process promotes the genetic and/or epigenetic changes required to complete the carcinogenic process. One possibility is that chronic exposure to reactive oxygen species (ROS) or other reactive products of inflammatory cells promotes further mutagenesis and genomic instability in initiated hepatocytes. Further evaluation of the genetic changes that occur in cells as they progress to malignancy will help to clarify the biochemical mechanisms responsible for tumor progression and identify targets for preventive strategies.

FUNDING

National Institutes of Health (R01 ES016313, P30 ES002109, P01 ES006052, P30 ES003819); The Center of Excellence on

Environmental Health, Toxicology and Management of Chemicals, Thailand (R.W.).

REFERENCES

Adams, W. T., and Skopek, T. R. (1987). Statistical test for the comparison of samples from mutational spectra. *J. Mol. Biol.* **194,** 391–396.

Busby, W. F., Jr., and Wogan, G. N. (1984). Aflatoxins. In *Chemical Carcinogens,* 2nd ed. (C. E. Searle, Ed.), pp. 945–1136. American Chemical Society, Washington, DC.

Cariello, N. F., Piegorsch, W. W., Adams, W. T., and Skopek, T. R. (1994). Computer program for the analysis of mutational spectra: Application to p53 mutations. *Carcinogenesis* **15,** 2281–2285.

Chen, T., Heflich, R. H., Moore, M. M., and Mei, N. (2010). Differential mutagenicity of aflatoxin B1 in the liver of neonatal and adult mice. *Environ. Mol. Mutagen.* **51,** 156–163.

Court, R., Cook, N., Saikrishnan, K., and Wigley, D. (2007). The crystal structure of lambda-Gam protein suggests a model for RecBCD inhibition. *J. Mol. Biol.* **371,** 25–33.

Dycaico, M. J., Stuart, G. R., Tobal, G. M., de Boer, J. G., Glickman, B. W., and Provost, G. S. (1996). Species-specific differences in hepatic mutant frequency and mutational spectrum among lambda/lacI transgenic rats and mice following exposure to aflatoxin B1. *Carcinogenesis* **17,** 2347–2356.

Egner, P. A., Groopman, J. D., Wang, J. S., Kensler, T. W., and Friesen, M. D. (2006). Quantification of aflatoxin-B1-N7-Guanine in human urine by high-performance liquid chromatography and isotope dilution tandem mass spectrometry. *Chem. Res. Toxicol.* **19,** 1191–1195.

El-Serag, H. B., and Rudolph, K. L. (2007). Hepatocellular carcinoma: Epidemiology and molecular carcinogenesis. *Gastroenterology* **132,** 2557–2576.

Furth, M. E., and Wickner, S. H. (1983). Lambda DNA replication. In *Lambda II* (R. W. Hendrix, J. W. Roberts, F. W. Stahl and R. A. Weisberg, Eds.), pp. 145–173. Cold Spring Harbor Press, Cold Spring Harbor, NY.

Futreal, P. A., Coin, L., Marshall, M., Down, T., Hubbard, T., Wooster, R., Rahman, N., and Stratton, M. R. (2004). A census of human cancer genes. *Nat. Rev. Cancer* **4,** 177–183.

Groopman, J.D., Kensler, T.W., and Wild, C.P. (2008). Protective Interventions to prevent aflatoxin-induced carcinogenesis in developing countries. *Annu. Rev. Public Health* **29**, 187–203.

Hayes, J. D., Judah, D. J., McLellan, L. I., and Neal, G. E. (1991). Contribution of the glutathione S-transferases to the mechanisms of resistance to aflatoxin B1. *Pharmacol. Ther.* **50,** 443–472.

He, G., Yu, G. Y., Temkin, V., Ogata, H., Kuntzen, C., Sakurai, T., Sieghart, W., Peck-Radosavljevic, M., Leffert, H. L., and Karin, M. (2010). Hepatocyte IKKbeta/NF-kappaB inhibits tumor promotion and progression by preventing oxidative stress-driven STAT3 activation. *Cancer Cell* **17,** 286–297.

Horiguchi, M., Masumura, K. I., Ikehata, H., Ono, T., Kanke, Y., and Nohmi, T. (2001). Molecular nature of ultraviolet B light-induced deletions in the murine epidermis. *Cancer Res.* **61,** 3913–3918.

Johnston, D. S., and Stone, M. P. (2000). Replication of a site-specific trans-8,9-dihydro-8-(N7-guanyl)-9-hydroxyaflatoxin B(1) adduct by the exonuclease deficient Klenow fragment of DNA polymerase I. *Chem. Res. Toxicol.* **13,** 1158–1164.

Levy, D. D., Groopman, J. D., Lim, S. E., Seidman, M. M., and Kraemer, K. H. (1992). Sequence specificity of aflatoxin B1-induced mutations in a plasmid replicated in xeroderma pigmentosum and DNA repair proficient human cells. *Cancer Res.* **52,** 5668–5673.

Maeda, S., Kamata, H., Luo, J. L., Leffert, H., and Karin, M. (2005). IKKbeta couples hepatocyte death to cytokine-driven compensatory proliferation that promotes chemical hepatocarcinogenesis. *Cell* **121,** 977–990.

Masumura, K., Matsui, K., Yamada, M., Horiguchi, M., Ishida, K., Watanabe, M., Ueda, O., Suzuki, H., Kanke, Y., Tindall, K. R., Wakabayashi, K., Sofuni, T., and Nohmi, T. (1999). Mutagenicity of 2-amino-1-methyl-6-phenylimidazo [4,5-b]pyridine (PhIP) in the new gpt delta transgenic mouse. *Cancer Lett.* **143,** 241–244.

Masumura, K., Matsui, K., Yamada, M., Horiguchi, M., Ishida, K., Watanabe, M., Wakabayashi, K., and Nohmi, T. (2000). Characterization of mutations induced by 2-amino-1-methyl-6-phenylimidazo[4,5-b]pyridine in the colon of gpt delta transgenic mouse: Novel G:C deletions beside runs of identical bases. *Carcinogenesis* **21,** 2049–2056.

Masumura, K., Totsuka, Y., Wakabayashi, K., and Nohmi, T. (2003). Potent genotoxicity of aminophenylnorharman, formed from non-mutagenic norharman and aniline, in the liver of gpt delta transgenic mouse. *Carcinogenesis* **24,** 1985–1993.

Naugler, W. E., Sakurai, T., Kim, S., Maeda, S., Kim, K., Elsharkawy, A. M., and Karin, M. (2007). Gender disparity in liver cancer due to sex differences in MyD88-dependent IL-6 production. *Science* **317,** 121–124.

Nohmi, T., Katoh, M., Suzuki, H., Matsui, M., Yamada, M., Watanabe, M., Suzuki, M., Horiya, N., Ueda, O., Shibuya, T., Ikeda, H., and Sofuni, T. (1996). A new transgenic mouse mutagenesis test system using Spi- and 6-thioguanine selections. *Environ. Mol. Mutagen.* **28,** 465–470.

Nohmi, T., Suzuki, M., Masumura, K., Yamada, M., Matsui, K., Ueda, O., Suzuki, H., Katoh, M., Ikeda, H., and Sofuni, T. (1999). Spi(-) selection: An efficient method to detect gamma-ray-induced deletions in transgenic mice. *Environ. Mol. Mutagen.* **34,** 9–15.

Preisler, V., Caspary, W. J., Hoppe, F., Hagen, R., and Stopper, H. (2000). Aflatoxin B1-induced mitotic recombination in L5178Y mouse lymphoma cells. *Mutagenesis* **15,** 91–97.

Refolo, L. M., Conley, M. P., Sambamurti, K., Jacobsen, J. S., and Humayun, M. Z. (1985). Sequence context effects in DNA replication blocks induced by aflatoxin B1. *Proc. Natl. Acad. Sci. U.S.A.* **82,** 3096–3100.

Reynolds, R., Witherspoon, S., and Fox, T. (2004). The infant mouse as an in vivo model for the detection and study of DNA damage-induced changes in the liver. *Mol. Carcinog.* **40,** 62–72.

Sengstag, C., Weibel, B., and Fasullo, M. (1996). Genotoxicity of aflatoxin B1: Evidence for a recombination-mediated mechanism in *Saccharomyces cerevisiae*. *Cancer Res.* **56,** 5457–5465.

Shupe, T., and Sell, S. (2004). Low hepatic glutathione S-transferase and increased hepatic DNA adduction contribute to increased tumorigenicity of aflatoxin B1 in newborn and partially hepatectomized mice. *Toxicol. Lett.* **148,** 1–9.

Singer, E. (1971). General recombination. In *The Bacteriophage Lambda* (A. D. Hershey, Ed.), pp. 139–174. Cold Spring Harbor Laboratory, Cold Spring Harbor, NY.

Smela, M. E., Hamm, M. L., Henderson, P. T., Harris, C. M., Harris, T. M., and Essigmann, J. M. (2002). The aflatoxin B(1) formamidopyrimidine adduct plays a major role in causing the types of mutations observed in human hepatocellular carcinoma. *Proc. Natl. Acad. Sci. U.S.A.* **99,** 6655–6660.

Smith, G. R. (1983). *General Recombination* (R. W. Hendrix, J. W. Roberts, F. W. Stahl and R.A.Weisberg, Eds.), pp. 175–209. Cold Spring Harbor Press, Cold Spring Harbor, NY.

Stettler, P. M., and Sengstag, C. (2001). Liver carcinogen aflatoxin B1 as an inducer of mitotic recombination in a human cell line. *Mol. Carcinog.* **31,** 125–138.

Vesselinovitch, S. D., Mihailovich, N., Wogan, G. N., Lombard, L. S., and Rao, K. V. (1972). Aflatoxin B1, a hepatocarcinogen in the infant mouse. *Cancer Res.* **32,** 2289–2291.

Woo, L. L., Egner, P. A., Belanger, C. L., Wattanawaraporn, R., Trudel, L. J., Croy, R. G., Groopman, J. D., Essigmann, J. M., and Wogan, G. N. (2011). Aflatoxin B1-DNA adduct formation and mutagenicity in livers of neonatal male and female B6C3F1 mice. *Toxicol. Sci.* **122,** 38–44.